nature cell biology

LETTERS

Yeast kinesin-8 depolymerizes microtubules in a length-dependent manner

Vladimir Varga[1], Jonne Helenius[1,2], Kozo Tanaka[3], Anthony A. Hyman[1], Tomoyuki U. Tanaka[3] and Jonathon Howard[1,4]

The microtubule cytoskeleton and the mitotic spindle are highly dynamic structures[1], yet their sizes are remarkably constant, thus indicating that the growth and shrinkage of their constituent microtubules are finely balanced[2,3]. This balance is achieved, in part, through kinesin-8 proteins (such as Kip3p in budding yeast and KLP67A in *Drosophila)* that destabilize microtubules[3–8]. Here, we directly demonstrate that Kip3p destabilizes microtubules by depolymerizing them — accounting for the effects of kinesin-8 perturbations on microtubule and spindle length observed in fungi and metazoan cells. Furthermore, using single-molecule microscopy assays[9], we show that Kip3p has several properties that distinguish it from other depolymerizing kinesins, such as the kinesin-13 MCAK[10,11]. First, Kip3p disassembles microtubules exclusively at the plus end and second, remarkably, Kip3p depolymerizes longer microtubules faster than shorter ones. These properties are consequences of Kip3p being a highly processive, plus-end-directed motor[12], both *in vitro* and *in vivo*. Length-dependent depolymerization provides a new mechanism for controlling the lengths of subcellular structures[13].

The cellular functions of kinesin-8 proteins are associated with their ability to destabilize microtubules. Deletion of kinesin-8 in budding yeast (Kip3p) and *Aspergillus* (KipB) makes these cells more resistant to microtubule depolymerizing drugs and leads to longer cytoplasmic microtubules[4,5,7]. This, in turn, leads to defects in the positioning of the mitotic spindle[4,7] that, in budding yeast, is thought to be mediated by pulling forces generated by shortening microtubules[4]. Mutants also have mitotic defects: the metaphase mitotic spindle is longer[6] and anaphase, which like spindle positioning is associated with microtubule shortening, is delayed[6,7]. Related defects are seen in *Drosophila*. RNA interference (RNAi) or mutation of the fly kinesin-8 (KLP67A) leads to longer metaphase spindles[14] and is associated with various mitotic and meiotic defects[15]. Conversely, overexpression of KLP67A leads to shorter metaphase spindles[3]. Thus, kinesin-8 proteins destabilize the microtubule cytoskeleton. This destabilizing activity is similar to that of kinesin-13 proteins whose depletion in *Xenopus* extracts leads to longer spindles[16] and overexpression in tissue culture cells leads to shorter cytoplasmic microtubules[17] and spindles[3].

Kinesin-13 proteins destabilize microtubules by depolymerizing them from their ends[10,11]. There are functional and evolutionary reasons to believe that kinesin-8 proteins do the same. First, as summarized above, perturbations of kinesin-8 proteins give similar (but not identical) phenotypes to kinesin-13 proteins. Second, kinesin-8 proteins are quite closely related to kinesin-13 proteins in the kinesin superfamily[18]. Moreover, because fungi have no kinesin-13 proteins, it has been hypothesized that kinesin-8 proteins could serve as the depolymerizing proteins in these organisms. However, the depolymerase activity of kinesin-8 has not been tested directly.

To determine whether budding yeast Kip3p is a microtubule depolymerase, the full-length His-tagged protein was expressed in insect cells, purified to homogeneity and its activity measured in sedimentation assays. When Kip3p was incubated with guanylyl(α,β)-methylenediphosphate (GMP–CPP)-stabilized microtubules and ATP for 25 min and centrifuged, most of the tubulin was found in the supernatant (see Supplementary Information, Fig. S1) indicating that the microtubules had depolymerized. Depolymerization depended on Kip3p because when it was omitted, most of the tubulin was found in the pellet. GMP–CPP microtubules were used because GMP–CPP (a slowly-hydrolysable analogue of GTP[19]) mimics the GTP found in the end cap of growing microtubules, where depolymerases are expected to act.

To determine how Kip3p depolymerizes microtubules, its activity was characterized in a microscope-based assay. In this assay, rhodamine-labelled microtubules were immobilized on a cover-slip using surface-adsorbed anti-tubulin antibodies and imaged using epifluorescence microscopy (Fig. 1a). After infusion of Kip3p and ATP, the microtubules depolymerized at rates up to 2 μm min^{-1} (Fig. 1b and see Supplementary Information, Movie 1). Kip3p also depolymerized taxol-stabilized microtubules (data not shown).

[1]Max Planck Institute of Molecular Cell Biology & Genetics, Pfotenhauerstr. 108, 01307 Dresden, Germany. [2]Current address: Center of Biotechnology, Dresden University of Technology, Tatzberg 47-51, 01307 Dresden, Germany. [3]School of Life Sciences, University of Dundee, Wellcome Trust Biocentre, Dundee DD1 5EH, UK. [4]Correspondence should be addressed to J.H. (e-mail: howard@mpi-cbg.de)

Received 9 May 2006; accepted 28 July 2006; published online 13 August 2006; DOI: 10.1038/ncb1462

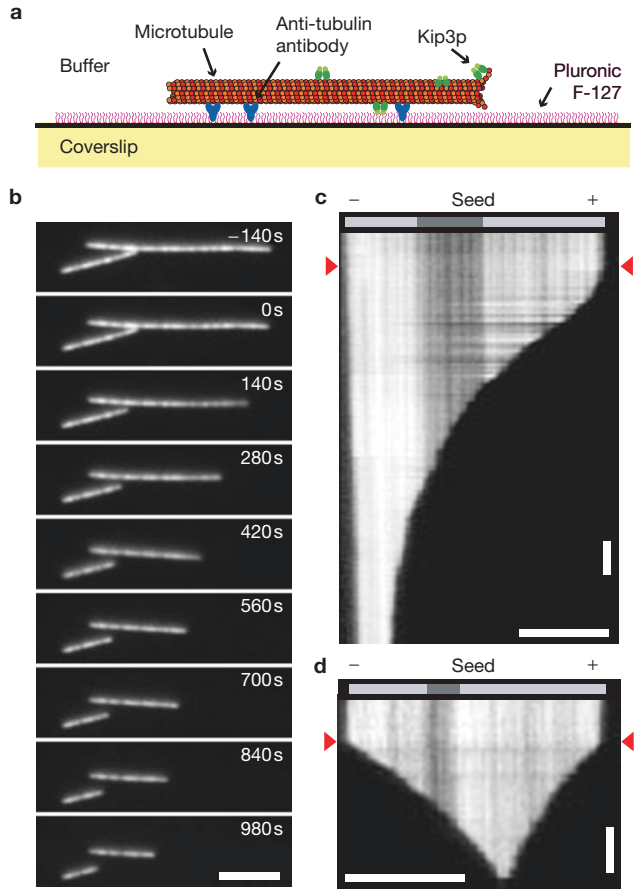

Figure 1 Kip3p-dependent microtubule depolymerization. (**a**) Schematic representation of the *in vitro* depolymerization assay depicting a microtubule (red) immobilized above the glass surface by anti-tubulin antibodies (blue). The copolymer Pluronic F-127 (magenta) was used to block the surface. (**b**) Epifluorescence microscopy images of immobilized microtubules recorded at 140 s intervals. Kip3p (6.2 nM) was added at $t = 0$. (**c**, **d**) Kymographs showing polarity-marked microtubules being depolymerized by Kip3p (**c**) and MCAK (**d**). Images were recorded at 10 s intervals. Red arrowheads indicate addition of 7 nM Kip3p and 2.5 nM MCAK. Horizontal scale bars represent 4 μm and vertical scale bars represent 2 min. Plus (+) and minus (–) symbols above the image refer to the polarity of the microtubule.

Kip3p depolymerized microtubules exclusively from one end (Fig. 1b and see Supplementary Information, Movie 1). Depolymerization at the other end was not distinguishable from the very slow spontaneous depolymerization of GMP–CPP microtubules (0.03 μm min^{-1}). To determine from which end depolymerization took place, the experiment was repeated with polarity-marked microtubules in which brightly labelled tubulin was grown onto dimly labelled seeds. Depolymerization took place exclusively from the end of the longer segment (Fig. 1), which corresponds to the plus end. Similar results were found in 45 of 50 polarity-marked microtubules, indicating that Kip3p is a plus-end depolymerizing kinesin (the small number of apparent exceptions is accounted for by microtubule breakage). The observation of exclusively plus-end depolymerization was surprising as kinesin-13 proteins depolymerize microtubules from both ends[10,11] (an example of MCAK-driven depolymerization is shown in Fig. 1d). Although MCAK acts at both ends, it depolymerizes the minus end 1.7 ± 0.2 times faster than the plus end (mean ± s.d., $n = 26$).

Measurement of the depolymerization rate induced by Kip3p was not straightforward because the rate varied between microtubules (Fig. 1b) and changed over time, even for an individual microtubule (Fig. 1c). To understand this variability, the lengths of several microtubules were measured over time after Kip3p was infused into the flow cell. The depolymerization rate initially increased and reached a maximum at a time after infusion that was longer for longer microtubules (Fig. 2a). Subsequently, the rate of depolymerization decreased. The maximum depolymerization rate was higher for longer microtubules than shorter ones (Fig. 2b) and showed no obvious saturation, even for microtubule lengths up to 10 μm. The slopes of the depolymerization rate versus microtubule-length curves increased as the Kip3p concentration was increased (Fig. 2b). We were unable to obtain depolymerization rates higher than 2 μm min^{-1} because the microtubules detached from the antibodies and diffused away from the surface at Kip3p concentrations above 10 nM. Depolymerization by Kip3p was very different to that by MCAK. The maximum depolymerization rate was reached at shorter times after infusing MCAK than Kip3p. For MCAK, the time to maximum depolymerization was the same for short and long microtubules (unlike Kip3p), the depolymerization rate changed little over time (Figs 1d, 2a; right curves) and the rate did not depend significantly on microtubule length (Fig. 2b). In summary, Kip3p, unlike MCAK, has a length-dependent depolymerization and this accounts for the observed variability in the rates of Kip3p-mediated depolymerization.

Length-dependent depolymerization may be due to longer microtubules having more Kip3p at their plus ends than shorter microtubules. To examine this possibility, the depolymerization assays were repeated using Kip3p tagged with GFP and total internal reflection fluorescence microscopy (TIRF)[9]. Two constructs differing in the position of Kip3p and GFP were prepared and expressed in insect cells. The proteins were subsequently purified and assayed for depolymerization activity. Both GFP-tagged proteins possessed microtubule depolymerizing activity comparable with non-GFP labelled protein and displayed length-dependent depolymerization. The GFP signal increased monotonically from the minus end to the plus end (Fig. 3a and see Supplementary Information, Movie 2), indicating that the number of Kip3p–GFP motors bound to the microtubule increased with distance towards the plus end. Line scans along the microtubule showed an approximately linear increase in fluorescence intensity (Fig. 3b). The slope was independent of the microtubule length, so longer microtubules did indeed have higher concentrations of Kip3p at their plus ends than shorter microtubules (Fig. 3b).

We then tested whether the observed accumulation of Kip3p towards the plus ends of microtubules was due to its motor activity. The concentration of Kip3p–GFP was reduced to 1 nM or less so that individual spots corresponding to single Kip3p–GFP molecules could be resolved on the microtubule lattice. These experiments showed that Kip3p–GFP is a slow and highly processive motor (Fig. 3c, d and see Supplementary Information, Movie 3). The speed was 3 μm min^{-1} (mode of >100 molecules in four experiments on three different Kip3p–GFP preparations; see Supplementary Information, Fig. S2) and independent of the position of Kip3p on the microtubule (Fig. 3d). Experiments with polarity-marked microtubules showed that movement was towards the plus end (data not shown). This speed and direction (which agree with earlier results on KLP67A, the *Drosophila* homologue of Kip3p[12]) classify Kip3p as a slow kinesin, like other mitotic kinesins such as Eg5 (kinesin-5) and CENP-E (kinesin-7), and unlike organelle transport kinesins, such as

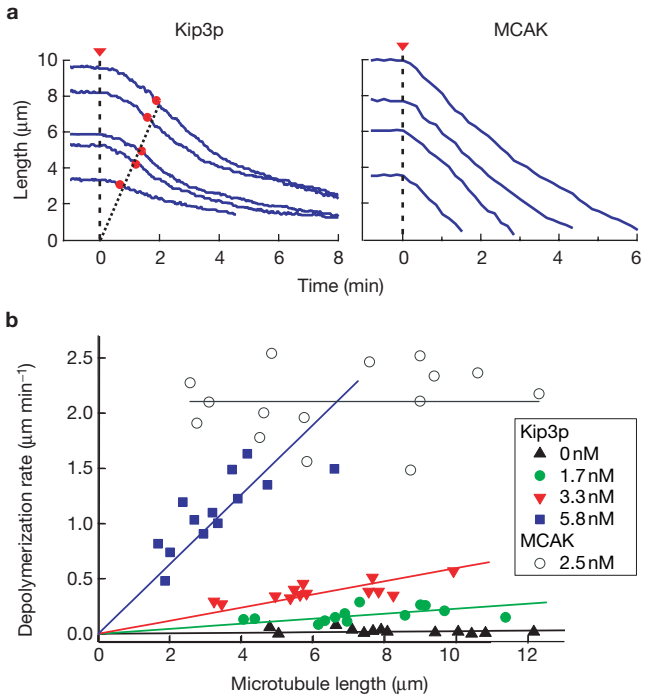

Figure 2 Comparison of microtubule depolymerization by Kip3p and MCAK. (**a**) Graphs of microtubule lengths against time, before and after addition of 7.5 nM Kip3p and 2.5 nM MCAK. Each curve represents a single microtubule and the red arrowheads indicate addition of depolymerase. The red dots on the Kip3p curves indicate times of maximum depolymerization rates. (**b**) Graph of the maximal rate of depolymerization versus microtubule length at the indicated concentrations of Kip3p and MCAK. Kip3p trend lines were fit using least squares forced through the origin. The MCAK trend line denotes the average depolymerization rate.

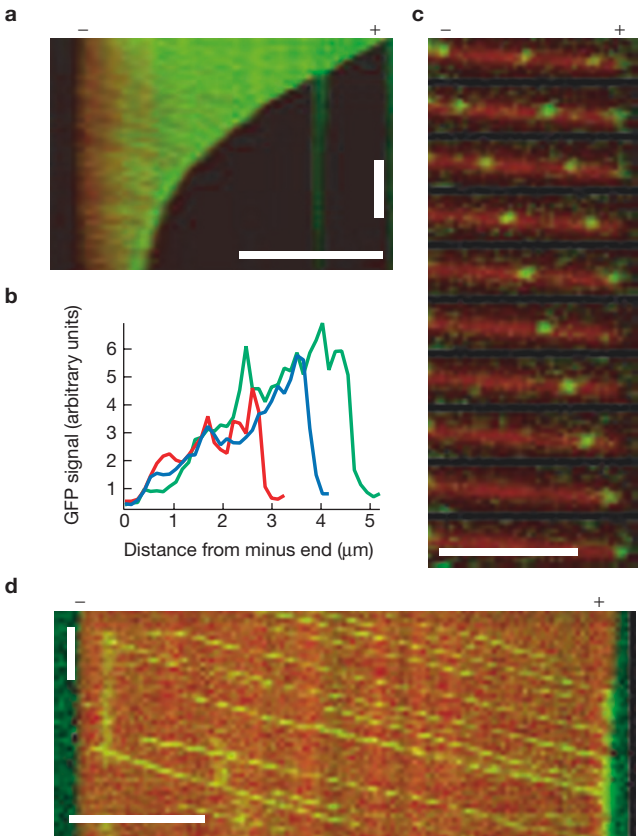

Figure 3 Kip3p is a highly processive plus-end directed motor that pauses at the plus ends of microtubules. (**a**) Dual-colour kymograph of a microtubule (red) in the presence of Kip3p–GFP (green; 5 nM). TIRF–FITC and TRITC epifluorescence microscopy images were recorded every 10 s. (**b**) Graph of the GFP intensity along the length of three microtubules (shown in different colours) in the presence of 9 nM Kip3p–GFP. A single TIRF–FITC image (to avoid bleaching the sample) was recorded after the lag phase. (**c**) TIRF–FITC images of Kip3p–GFP molecules (green) were overlaid on TRITC epifluorescence microscopy images of the microtubule (red). The images were recorded at 10 s intervals. (**d**) Kymograph showing movement of single molecules of Kip3p–GFP (green) along the lattice of microtubule (red). Both TIRF–FITC and epifluorescence images were recorded at 10 s intervals. Horizontal scale bars represent 4 μm and vertical bars 2 min. Plus (+) and minus (–) symbols above the image refer to the polarity of the microtubule.

KHC (kinesin-1) and KIF1 (kinesin-3), which move more than ten times faster[20]. The average distance moved by single Kip3p–GFP molecules before dissociating from the lattice was 12.4 ± 2.3 μm (mean ± s.e.m. from three independent experiments, $n = 29$ dissociations), as determined by dividing the total distance moved by the 29 dissociations that occurred before Kip3p molecules reached the end of the microtubule. When at the end of the microtubule, single Kip3p molecules remained there for up to 1 min (0.5 ± 0.2 min; mean ± s.d. from three independent experiments, $n = 23$). Assuming that Kip3p makes 8-nm steps like other kinesins[20], this processivity corresponds to an average run of 1500 steps — twenty times larger than for kinesin-1 (ref. 21) and myosin V (ref. 22). Thus Kip3p is the most processive cytoskeletal motor protein characterized to date.

The highly processive plus-end-directed motility of Kip3p accounts for the observed length-dependent plus-end depolymerization. Assuming that Kip3p binds equally well anywhere along the microtubule lattice, the total amount of Kip3p binding to the microtubule will be proportional to its length. Because Kip3p walks processively towards the plus end, rarely unbinding, a linear Kip3p concentration gradient is expected, with the concentration increasing from zero at the minus end to a value proportional to microtubule length at the plus end, as we observed. The microtubule therefore acts as an antenna that funnels Kip3p molecules to its plus end. The high processivity and low speed also accounts for the lag seen between infusion of Kip3p and attainment of the maximum depolymerization rate observed in Fig. 2a — it takes a time approximately equal to the microtubule length divided by the speed of movement to establish the steady-state intensity profile. This time is in agreement with the length-dependent lag observed in Fig. 2a where the dotted line has a slope of 3.6 μm min^{-1}, approximately equal to the speed of Kip3p–GFP.

To link our *in vitro* observations to the cellular properties of Kip3p, the behaviour of GFP-tagged Kip3p in yeast cells was studied. A Kip3p–4GFP fusion protein was made by inserting four tandem copies of the gene encoding *GFP* into the original *KIP3* locus. The fusion protein was functional as nuclei translocated normally into the bud during mitosis, in contrast with *kip3*-deleted cells[2]. Cells were arrested in metaphase by depletion of *CDC20*, which encouraged formation of long nuclear microtubules in elongated nuclei formed by the back-and-forth motion of the spindle[23]. In these cells, small spots of Kip3p–4GFP could be observed moving along nuclear microtubules (Fig. 4a, b and see Supplementary Information, Fig. S3 and Movies 4, 5) at a rate of 2.8 ± 1.0 μm min^{-1} (mean ± s.d., $n = 27$). These GFP signals were moving away from the spindle towards the distal microtubule ends,

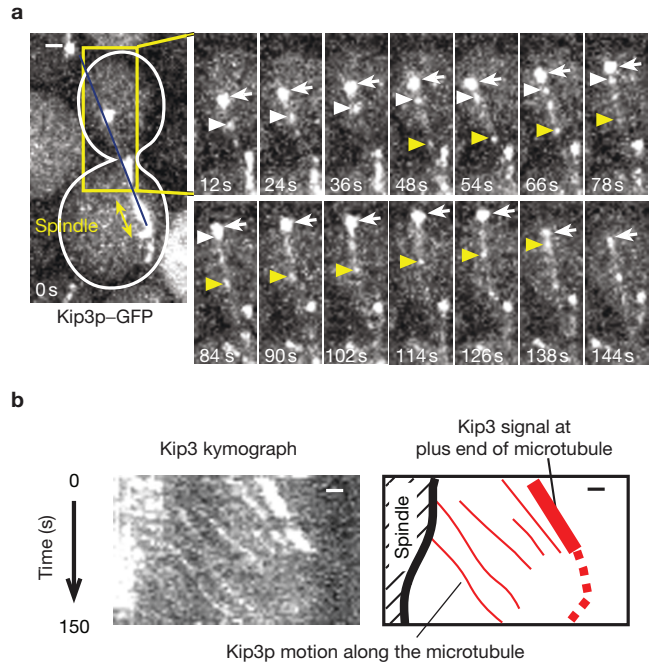

Figure 4 Kip3p is a highly persistent plus-end-directed motor *in vivo*. (**a**) Kip3p motion along a microtubule. Kip3p–4GFP signals are shown at representative times. White arrows show the position of Kip3p–4GFP signals at the microtubule plus end (microtubules were labelled with CFP, data not shown). White and yellow arrowheads indicate the position of each Kip3p–4GFP signal along the microtubule. Time corresponds to that in the kymograph below. The cell shape is outlined in white in the left panel. (**b**) The kymograph shows that Kip3p–4GFP signals (along the blue line in **a**) move towards the microtubule plus end. The schematic representation shows the tracking of Kip3p–4GFP signals along the microtubule (red thin lines). The scale bars represent 1 μm.

suggesting plus-end directed motion of Kip3p. CEN3 labelled with CFP (data not shown and ref. 23) was captured by the microtubule shown in Fig. 4 (data not shown), confirming that the microtubule was nuclear. Kip3p motion towards the microtubule plus end was also observed along cytoplasmic microtubules (data not shown). The motion was very persistent and even the dimmest GFP spots usually reached the microtubule ends. The similarities between the speed, direction and persistence of Kip3p motion *in vivo* and *in vitro* indicates that, in cells, Kip3p is responsible for its own transport along microtubules, rather than being carried by another motor. Because their speed was faster than the microtubule growth rate of 1.4 ± 0.4 μm min^{-1} (ref. 23), Kip3p spots always caught up with the ends of growing microtubules, leading to bright plus-end labelling (Fig. 4). When at the end, the Kip3 signal remained at the growing end of the microtubule. However, during shrinkage of the microtubules, Kip3 signals were markedly reduced (Fig. 4). Such Kip3p behaviour is similar to that of microtubule plus-end-tracking proteins (+TIPs)[24].

We have shown that Kip3p is a microtubule depolymerase *in vitro*. This enzymatic activity is in agreement with the ability of Kip3p to destabilize microtubules *in vivo* and accounts, at least qualitatively, for the effects of kinesin-8 perturbations on microtubule and spindle lengths — interfering with kinesin-8 leads to longer microtubules and spindles[4–7], whereas overexpressing it leads to shorter spindles[3]. The high processivity allows Kip3p to efficiently target plus ends *in vivo* as observed, because no matter where it binds on the microtubule it will reach the end.

Depolymerization activity, on its own, cannot quantitatively explain how cells control the lengths of their microtubules. Isolated microtubules are highly dynamic polymers whose growing plus ends switch stochastically between growing and shrinking phases. This stochasticity leads to a very broad length distribution[20]. A depolymerase is expected to increase the catastrophe rate (the transition from growth to shrinkage) by depolymerizing the stabilizing GTP cap at the growing end[25], but this will only decrease the average microtubule length and not the relative spread of lengths. Length-dependent depolymerase activity of the type that we have discovered for Kip3p can change this in two possible ways. First, it may lead to a length-dependent catastrophe rate and a corresponding decrease in the relative spread of the length distribution, because longer microtubules will accumulate more depolymerase than shorter microtubules at their growing ends. Interestingly, higher catastrophe rates for longer microtubules have been observed in *Xenopus* egg extracts[26], suggesting the possible action of a length-dependent depolymerase. Second, other proteins (such the +TIPs EB1 or CLIP-170, ref. 24) may completely suppress catastrophes. In this case a length-dependent depolymerase, by antagonizing such polymerases, would lead to a precisely defined microtubule length at which the end concentration of the depolymerase equals a threshold, such that depolymerization exactly balances growth. This length is equal to the growth rate divided by the slope of the depolymerization rate versus length curve. For typical microtubule growth rates of ~1 μm min^{-1}, and our measured slope of ~0.1 min^{-1} at nanomolar Kip3p concentrations (Fig. 2b), the set-point for microtubule length will be in the order of 10 μm, which is of the same order of magnitude of the lengths of microtubules in yeast and metazoans. Thus, a length-dependent depolymerase, together with growth-promoting proteins, can lead to the precise control of microtubule length.

Our finding that Kip3p is a highly processive motor and length-dependent depolymerase provides a mechanism for precisely controlling microtubule length. It has been proposed that the length of the metaphase spindle in *Drosophila* S2 cells is determined by coupling the sliding forces generated within the spindle and depolymerization rates[3]. If the *Drosophila* kinesin-8 is a length-dependent depolymerase like Kip3p, then it may participate in an alternative length-control mechanism that does not rely on spindle forces. Furthermore, a processive depolymerase could allow cells to selectively control the dynamics of different populations of microtubules. Because kinesin-8 molecules accumulate more at the ends of longer microtubules than shorter ones, the depolymerase activity may reach a threshold only in structures containing long stable microtubules. This may account for the larger effect of kinesin-8 perturbation on the more stable metaphase spindle compared with the more dynamic astral microtubules in *Drosophila* S2 cells[3]. It may also account for the difference in phenotypes between kinesin-8, which primarily affects spindle length, compared with kinesin-13, which affects the lengths of both spindle and astral microtubules[3]. Thus, our findings suggest new models for the regulation of the size of microtubule-based structures.

In conclusion, we have shown that Kip3p is a processive motor and depolymerase. This adds to the list of kinesin-related proteins that both move directionally on microtubules and alter their stability (kinesin-4, ref. 27; kinesin-14, ref. 28). The activities of Kip3p have interesting structural implications — they imply that the conserved motor domains that define the kinesin superfamily of proteins can be used either for processive motility (such as in kinesin-1, a motor but not a depolymerase) or for depolymerization (such as MCAK, which is a depolymerase but not

a motor), or for both (such as Kip3p). Separating the depolymerase and motor activities of Kip3p will be the key to examining whether length-dependent depolymerization is a length-control mechanism *in vivo*. □

Note added in proof: a related manuscript by Gupta et al. *(*Nature Cell Biol. ***8****, doi: 10.1038/ncb1457; 2006) is also published in this issue.*

METHODS

Kip3p expression. The coding region of *KIP3* was PCR amplified from a *Saccharomyces cerevisiae* cDNA library and cloned into the pFastBacM 13 vector. 6×His–Kip3p, 6×His–Kip3–eGFP and 6×His–eGFP–Kip3 were expressed in Sf9 cells (BAC-TO-BAC expression system; Invitrogen, Paisley, UK). Proteins were purified by cation exchange chromatography followed by metal-chelating chromatography (see Supplementary Information, Methods). Most experiments with Kip3p–GFP were performed using freshly purified protein because frozen protein formed aggregates that hinder single molecule analysis. The concentration of active Kip3p was determined using a filter-based ATP binding assay[11]. Kip3p concentrations are for the dimer. Human full-length His-tagged MCAK was expressed and purified as previously described[9]. MCAK concentrations are also for the dimer. Reagents were purchased from Sigma (St Louis, MO) unless indicated otherwise.

GMP–CPP microtubules. Porcine brain tubulin was purified and rhodamine-labeled (TAMRA, Invitrogen) as previously described[11]. GMP–CPP microtubules were assembled in BRB80 (80 mM PIPES–KOH at pH 6.9, 1 mM $MgCl_2$ and 1 mM EGTA) plus 1 mM MgGMP–CPP (Jena Bioscience, Jena, Germany) containing 0.5 μM rhodamine-labelled and 1.5 μM unlabelled tubulin dimer[11], incubated for 2 h at 37 °C, pelleted in an Airfuge (28 psi for 5 min; Beckman-Coulter, Fullerton, CA) and resuspended in BRB80 to a 0.2 μM tubulin-dimer concentration. To prepare polarity-marked microtubules, dimly labelled seeds were first assembled: 0.25 μM of rhodamine-labelled and 1.75 μM unlabelled tubulin dimer were incubated in BRB80 with 1 mM MgGMP–CPP for 20 min at 37 °C, pelleted in an Airfuge and resuspended in the reaction mixture used for preparation of normal rhodamine-labelled microtubules. After 40 min incubation at 37 °C, the microtubules were pelleted in an Airfuge and resuspended in BRB80 to 0.1 μM tubulin-dimer concentration. Key experiments were repeated with microtubules stabilized with 10 μM taxol.

Imaging. Microtubules and GFP-labelled Kip3p were imaged using a Zeiss Axiovert 200M microscope (Carl Zeiss, Göttingen, Germany) with a Zeiss 100× 1.45 αPlan-FLUAR objective. Images were acquired with either a Metamorph (Molecular Devices Corporation, Sunnyvale, CA) software-driven MicroMAX:512BFT CCD camera (Roper Scientific, Trenton, NJ) or an ImageQ software-driven Andor DV887 iXon camera (Andor Technology, Belfast, UK). Fluorescence excitation was provided by a mercury arc lamp coupled through an optical fiber and by a multi-line Coherent Innova 90 laser (Evergreen Laser Corporation, Durham, CT) coupled to a dual port TIRF condenser (Till Photonics, Gräfelfing, Germany) or by a single-line argon lase (161LGS; LG Laser Technology, Koheras, Kleinostheim, Germany) coupled to a prototype VisiTIRF condensor (Visitron Systems, Puchheim, Germany). FITC and TRITC filter sets (Chroma Technology Corp, Rockingham, VT) were used to image GFP and TAMRA fluorophores, respectively. TIRF illumination was performed at λ = 488 nm. The exposure time was 100 ms.

Microscope chambers. Microscope chambers were constructed using two silanized cover-slips separated by double-stick tape (Scotch 3M, St Paul, MN) such that channels 0.1 mm thick, 3 mm wide and 18 mm long were formed. Before silanization, 18 × 18 and 22 x 22 mm cover-slips (#1.5, Corning, Acton, MA) were extensively cleaned by immersion in different solutions in the following order: 55 min in acetone, 10 min in ethanol, 1 min nano-pure water, 60 min in Piranha solution (3:5 H_2O_2:H_2SO_4), three 1 min water rinses, 0.1 M KOH and finally two 1 min water rinses before drying in nitrogen. Following silanization for 1 h in 0.05% dichlorodimethylsilane in trichloroethylene, cover-slips were washed four times in methanol with sonication. After three further rinses with nano-pure water, silanized cover-slips were stored dry.

***In vitro* depolymerization assay.** Due to its smaller size, the top cover-slip (18 × 18 mm) allowed solutions to be added to and exchanged in the channels. To immobilize microtubules to cover-slips, channels were incubated with a series of buffers. First, a tubulin antibody (0.4% SAP.4G5 clone) in PBS was incubated for 5 min, followed by a 5 min incubation with 1% Pluronic F-127 in BRB80 and finally GMP–CPP microtubules in BRB80 were allowed to bind to the surface for 15 min. Channels were rinsed once with BRB80 before the reaction solutions were added. These solutions were typically BRB80 supplemented with 112.5 mM KCl, 0.1 mg ml^{-1} BSA, 1 mM ATP, anti-fade consisting of 1% β-mercaptoethanol, 40 mM glucose, 40 μg ml^{-1} glucose oxidase, 16 μg ml^{-1} catalase and various concentrations of Kip3p. The MCAK depolymerization assay was previously described[9].

Imaging analysis. Metamorph was used for simple image processing, including microtubule length measurements. A version of the Motion Tracking software package, written in the Pluk software development environment, was used to locate and track Kip3p–GFP molecules[9]. At Kip3p–GFP concentrations of 1 nM and less, individual GFP spots were resolved spatially and attributed to single Kip3p molecules based on their similar intensity to single kinesin–GFP and MCAK–GFP molecules[9].

Kip3p visualization *in vivo*. Kip3, microtubules and centromere (CEN3) capture were visualized in yeast strain *PMET3–CDC20 KIP3–4GFP CFP–TUB1 PGAL–CEN3–tetOs TetR–3ECFP* (T3981) as described previously [23,29,30]. Yeast cells were observed in a Deltavision microscope (Applied Precision, Issaquah, WA) using the JP4 filter set (Chroma) to discriminate GFP from CFP signals. Every 3 s, five *z*-sections (0.7 μm apart) were acquired and subsequently deconvoluted and projected to two-dimensional images using SoftWoRx software (Applied Precision).

Note: Supplementary Information is available on the Nature Cell Biology website.

ACKNOWLEDGEMENTS

We thank R. Ciosk, J.E. Harber, K. Nasmyth, E. Schiebel, R. Tsien, F. Uhlmann and M. van Breugel for reagents, G. Brouhard, S. Diez, D. Drechsel, R. Hartman and Y. Kitamura for technical help, Y. Kalaidzidis for the motion tracking program, and V. Bormuth, G. Brouhard, S. Endow, E. Schaeffer and J. Stear for comments on an earlier draft of this manuscript. V.V., J.H., A.A.H. and J.H. were supported by the Max Planck Society and the National Institutes of Health. K.T. and T.T. were supported by Cancer Research UK, The Wellcome Trust, Human Frontier Science Program and a Lister Research Prize.

COMPETING FINANCIAL INTERESTS

The authors declare that they have no competing financial interests.

Published online at http://www.nature.com/naturecellbiology/
Reprints and permissions information is available online at http://npg.nature.com/reprintsandpermissions/

1. Inoue, S. & Salmon, E. D. Force generation by microtubule assembly/disassembly in mitosis and related movements. *Mol. Biol. Cell* **6,** 1619–1640 (1995).
2. Hildebrandt, E. R. & Hoyt, M. A. Mitotic motors in *Saccharomyces cerevisiae. Biochim. Biophys. Acta* **1496,** 99–116 (2000).
3. Goshima, G., Wollman, R., Stuurman, N., Scholey, J. M. & Vale, R. D. Length control of the metaphase spindle. *Curr. Biol.* **15,** 1979–1988 (2005).
4. Cottingham, F. R. & Hoyt, M. A. Mitotic spindle positioning in *Saccharomyces cerevisiae* is accomplished by antagonistically acting microtubule motor proteins. *J. Cell Biol.* **138,** 1041–1053 (1997).
5. Miller, R. K. *et al*. The kinesin-related proteins, Kip2p and Kip3p, function differently in nuclear migration in yeast. *Mol. Biol. Cell* **9,** 2051–2068 (1998).
6. Straight, A. F., Sedat, J. W. & Murray, A. W. Time-lapse microscopy reveals unique roles for kinesins during anaphase in budding yeast. *J. Cell Biol.* **143,** 687–694 (1998).
7. Rischitor, P. E., Konzack, S. & Fischer, R. The Kip3-like kinesin KipB moves along microtubules and determines spindle position during synchronized mitoses in *Aspergillus nidulans* hyphae. *Eukaryot. Cell* **3,** 632–645 (2004).
8. West, R. R., Malmstrom, T., Troxell, C. L. & McIntosh, J. R. Two related kinesins, klp5+ and klp6+, foster microtubule disassembly and are required for meiosis in fission yeast. *Mol. Biol. Cell* **12,** 3919–3932 (2001).
9. Helenius, J., Brouhard, G., Kalaidzidis, Y., Diez, S. & Howard, J. The depolymerizing kinesin MCAK uses lattice diffusion to rapidly target microtubule ends. *Nature* **441,** 115–119 (2006).
10. Desai, A., Verma, S., Mitchison, T. J. & Walczak, C. E. Kin I kinesins are microtubule-destabilizing enzymes. *Cell* **96,** 69–78 (1999).

11. Hunter, A. W. *et al.* The kinesin-related protein MCAK is a microtubule depolymerase that forms an ATP-hydrolyzing complex at microtubule ends. *Mol. Cell* **11,** 445–457 (2003).
12. Pereira, A. J., Dalby, B., Stewart, R. J., Doxsey, S. J. & Goldstein, L. S. Mitochondrial association of a plus end-directed microtubule motor expressed during mitosis in *Drosophila*. *J. Cell Biol.* **136,** 1081–1090 (1997).
13. Marshall, W. F. Cellular length control systems. *Annu. Rev. Cell Dev. Biol.* **20,** 677–693 (2004).
14. Goshima, G. & Vale, R. D. The roles of microtubule-based motor proteins in mitosis: comprehensive RNAi analysis in the *Drosophila* S2 cell line. *J. Cell Biol.* **162,** 1003–1016 (2003).
15. Savoian, M. S., Gatt, M. K., Riparbelli, M. G., Callaini, G. & Glover, D. M. *Drosophila* Klp67A is required for proper chromosome congression and segregation during meiosis I. *J. Cell Sci.* **117,** 3669–3677 (2004).
16. Walczak, C. E., Mitchison, T. J. & Desai, A. XKCM1: a *Xenopus* kinesin-related protein that regulates microtubule dynamics during mitotic spindle assembly. *Cell* **84,** 37–47 (1996).
17. Maney, T., Wagenbach, M. & Wordeman, L. Molecular dissection of the microtubule depolymerizing activity of mitotic centromere-associated kinesin. *J. Biol. Chem.* **276,** 34753–34758 (2001).
18. Lawrence, C. J., Malmberg, R. L., Muszynski, M. G. & Dawe, R. K. Maximum likelihood methods reveal conservation of function among closely related kinesin families. *J. Mol. Evol.* **54,** 42–53 (2002).
19. Hyman, A. A., Salser, S., Drechsel, D. N., Unwin, N. & Mitchison, T. J. Role of GTP hydrolysis in microtubule dynamics: information from a slowly hydrolyzable analogue, GMPCPP. *Mol. Biol. Cell* **3,** 1155–1167 (1992).
20. Howard, J. *Mechanics of Motor Proteins and the Cytoskeleton*. **367** (Sinauer Associates, Sunderland, MA, 2001).
21. Vale, R. D. *et al.* Direct observation of single kinesin molecules moving along microtubules. *Nature* **380,** 451–453 (1996).
22. Sakamoto, T., Amitani, I., Yokota, E. & Ando, T. Direct observation of processive movement by individual myosin V molecules. *Biochem. Biophys. Res. Commun.* **272,** 586–590 (2000).
23. Tanaka, K. *et al.* Molecular mechanisms of kinetochore capture by spindle microtubules. *Nature* **434,** 987–994 (2005).
24. Akhmanova, A. & Hoogenraad, C. C. Microtubule plus-end-tracking proteins: mechanisms and functions. *Curr. Opin. Cell Biol.* **17,** 47–54 (2005).
25. Howard, J. & Hyman, A. A. Dynamics and mechanics of the microtubule plus end. *Nature* **422,** 753–758 (2003).
26. Dogterom, M., Felix, M. A., Guet, C. C. & Leibler, S. Influence of M-phase chromatin on the anisotropy of microtubule asters. *J. Cell Biol.* **133,** 125–140 (1996).
27. Bringmann, H. *et al.* A kinesin-like motor inhibits microtubule dynamic instability. *Science* **303,** 1519–1522 (2004).
28. Sproul, L. R., Anderson, D. J., Mackey, A. T., Saunders, W. S. & Gilbert, S. P. Cik1 targets the minus-end kinesin depolymerase kar3 to microtubule plus ends. *Curr. Biol.* **15,** 1420–1427 (2005).
29. Bressan, D. A., Vazquez, J. & Haber, J. E. Mating type-dependent constraints on the mobility of the left arm of yeast chromosome III. *J. Cell Biol.* **164,** 361–371 (2004).
30. Maekawa, H., Usui, T., Knop, M. & Schiebel, E. Yeast Cdk1 translocates to the plus end of cytoplasmic microtubules to regulate bud cortex interactions. *EMBO J.* **22,** 438–449 (2003).

Supplementary material

The yeast kinesin-8 Kip3p is a highly processive motor that depolymerizes microtubules in a length-dependent manner

Varga, et. al.

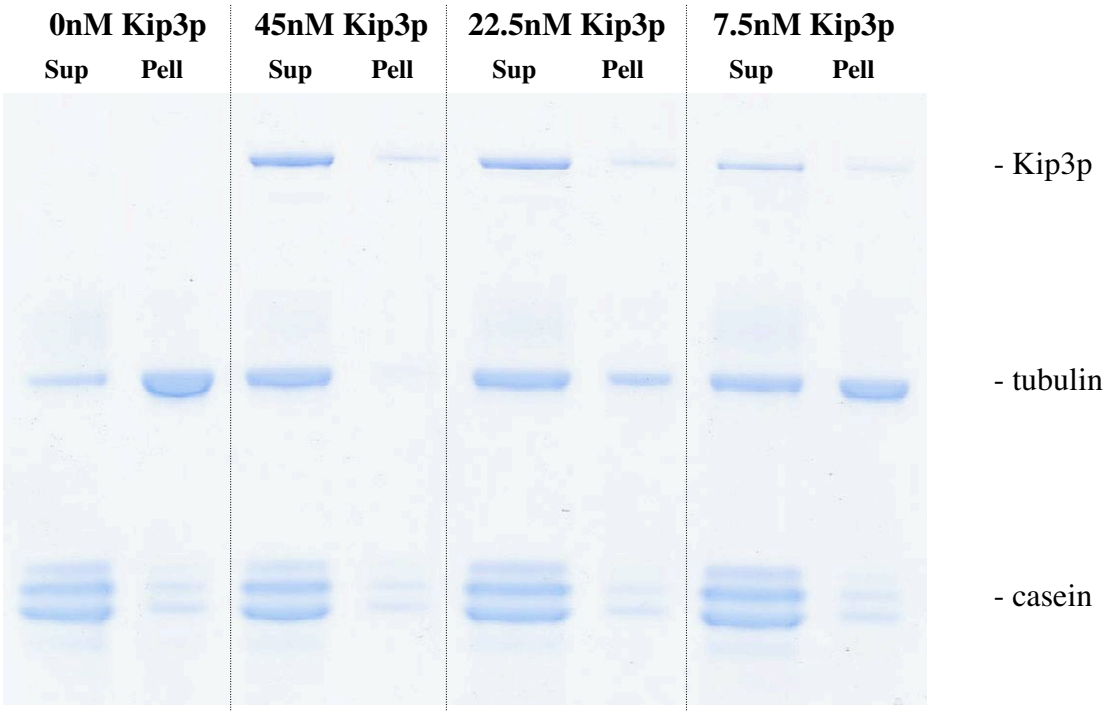

Supplementary Figure 1 | Microtubule sedimentaion assay showing that Kip3p is a microtubule depolymerase. GMP-CPP-stabilized microtubules were assembled for 2 hours at 37ºC in BRB80 plus 1mM MgGMP-CPP containing 5.4 μM tubulin dimer. Subsequently, microtubules and free tubulin were separate by centrifugation in an Airfuge (Beckman, 28 psi, 5min). The microtubule pellet was re-suspended in BRB 80 plus 112.5 mM KCl, 1 mM ATP and casein (final concentration 0.1 mg ml^{-1}) to a 0.5 μM tubulin dimer concentration. Microtubules were incubated with different concentrations of Kip3p for 25 minutes at room temperature and pelleted in an Airfuge. Supernatant and pellet were analyzed by SDS-PAGE.

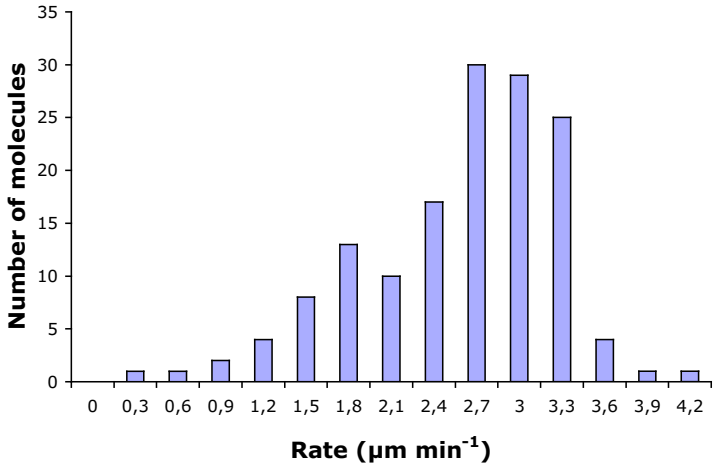

Supplementary Figure 2 | Speed distribution of single Kip3p molecules.
The motion tracking software package[S1] was used to locate Kip3p molecules in each frame of a time-lapse acquisition. Subsequently, the movement of each molecule was tracked in successive frames. The speed was determined by dividing the total distance traveled by the track duration. The minimum track duration was 40 s (four frames). Plotted are the frequency of rate observed in four independent experiments, representing 146 tracked molecules.

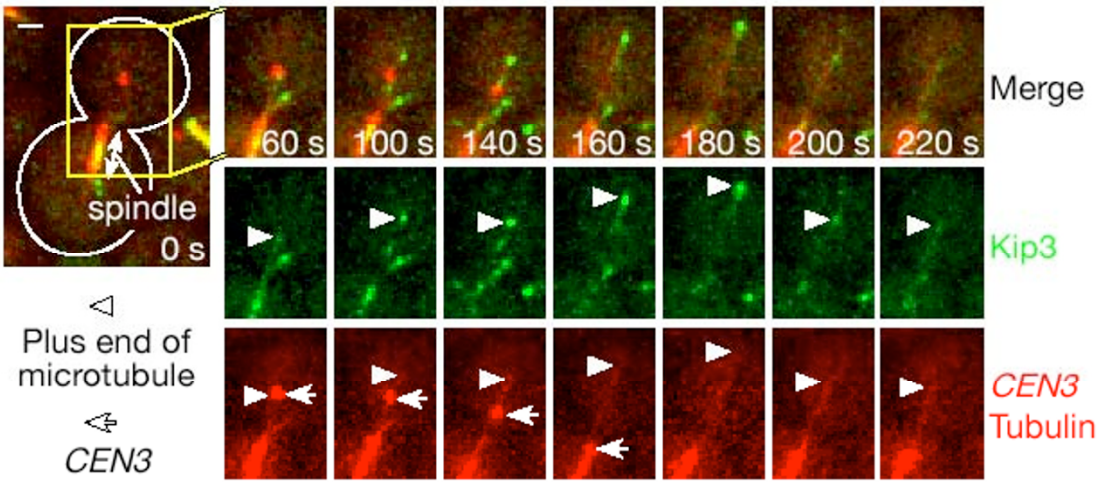

Supplementary Figure 3 | Kip3p behaves like a microtubule plus-end-tracking protein in vivo. A representative time-lapse image sequence of Kip3p-4GFP signals. *PMET3-CDC20 KIP3-4GFP CFP-TUB1 PGAL-CEN3-tetOs TetR-3ECFP* yeast cells (T3981) were arrested in metaphase and *CEN3* was activated as previously described[30]. Both GFP (Kip3p, green) and CFP (*CEN3* and α–tubulin, red) signals were collected every 20 seconds. White arrowheads show the plus end of a microtubule. White arrows indicate the position of *CEN3*. Zero time is set arbitrarily for the first panel, in which the cell shape is outlined in white. Scale bar denotes 1 µm. See Supplementary Video 5.

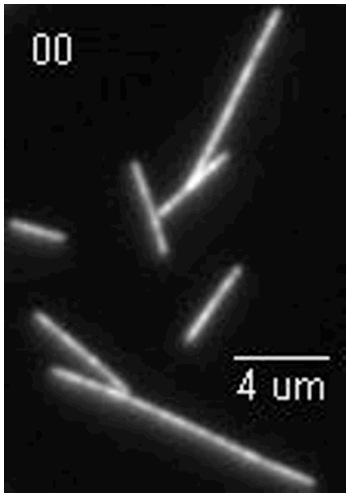

Supplementary Video 1 | Kip3p dependent microtubule depolymerization. Epifluorescence images (TRITC) of immobilized microtubules were recorded at 10 s intervals for 20 minutes. At 140 s, buffer containing 6.2 nM Kip3p was added. Video playback is 150x real-time.

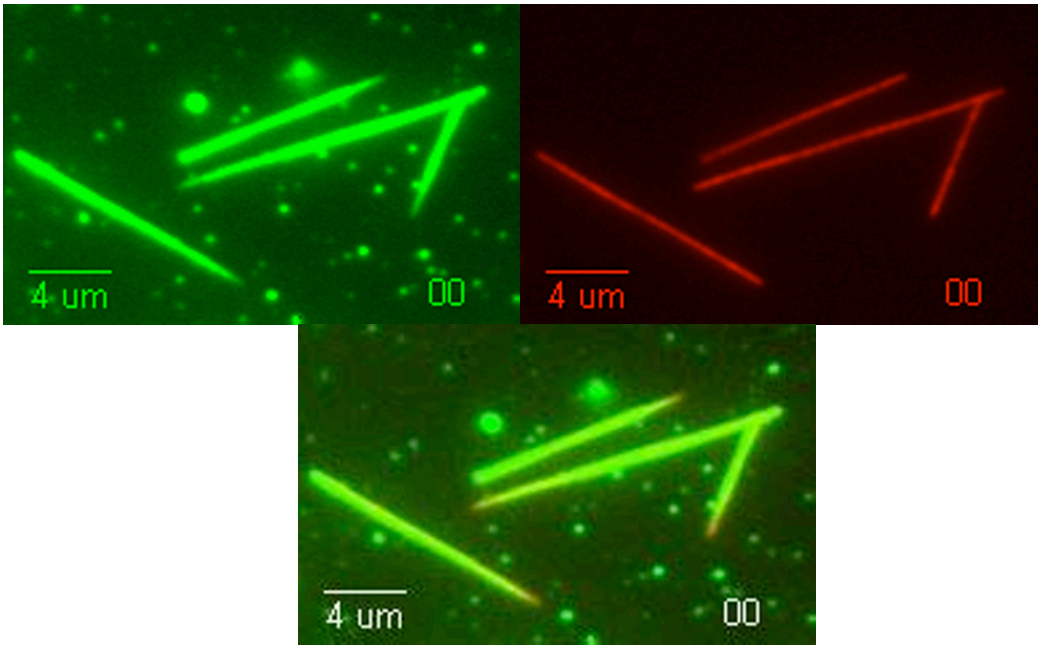

Supplementary Video 2 | Depolymerization of microtubules by Kip3p-GFP. Immobilized microtubules (red) in buffer containing 5 nM Kip3p-GFP (green). Both TIRF (FITC) and epifluorescence (TRITC) image were recorded at 10 s intervals and overlaid. Video playback is 75x real-time.

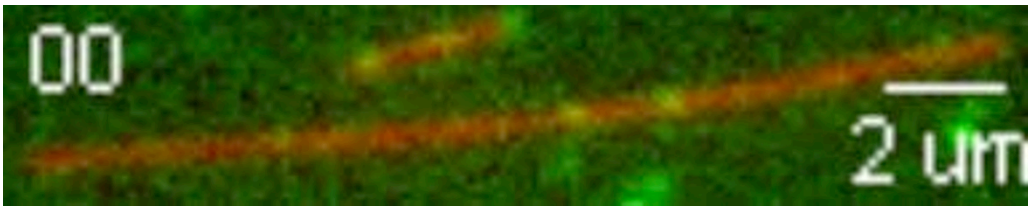

Supplementary Video 3 | Kip3p moves unidirectionally along microtubules and is highly processive. Immobilized microtubules (red) in buffer containing 0.2 nM Kip3p-GFP (green). Both TIRF (FITC) and epifluorescence (TRITC) image were recorded in 10 s intervals and overlaid. Video playback is 75x real-time.

Supplementary Video 4 | Kip3p is a highly persistent plus-end directed motor in vivo. Video of the cell shown in Figure 4. Speed in the movie is 30 times faster than the actual motion.

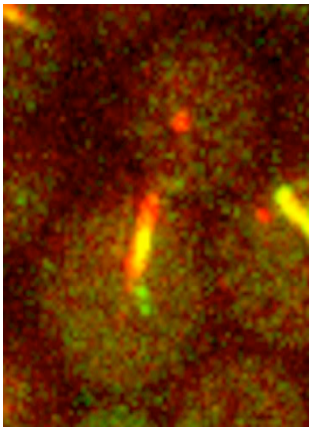

Supplementary Video 5 | Kip3p behaves like microtubule plus-end-tracking protein in vivo. Video of the cell shown in Supplementary Figure 3. Speed in the movie is 100 times faster than the actual motion.

Protein Purification Details

Sf9+ cells expressing protein were harvested by centrifugation (1,300 RPM, 5 min) and dissolved in cold lysis buffer (50 mM HEPES pH 7.5, 150 mM NaCl, 5% glycerol, 0.1% Tween 20, 1.5 mM $MgCl_2$, 3 mM EGTA, 1 mM DTT, 0.5 mM Mg-ATP, protease inhibitors [1 mM PMSF, 10 μg ml^{-1} antipain, 5 μg ml^{-1} chymotrypsin, 20 μg ml^{-1} TPCK, 2 μg ml^{-1} aprotinin, 0.7 μg ml^{-1} pepstatin A, 0.5 μg ml^{-1} leupeptin, 20 μg ml^{-1} TAME, 1 mM benzamidine, 10 μM E64]). Typically 4 ml of lysis buffer was used for 1 g of pellet. The crude lysate was clarified by centrifugation (50,000 x g, 20 min) and loaded onto a SP-sepharose column (Amersham Biosciences HiTrap SP-HP). The column was washed with cation buffer (20 mM HEPES-KOH pH 7.5, 150 mM NaCl, 1.5 mM $MgCl_2$, 1 mM DTT, 10 μM Mg-ATP, protease inhibitors), and the protein was eluted from the column with a continuous salt gradient (150 mM—1 M NaCl) using a BioCAD SPRINT system. Peak fractions were pooled, the buffer was exchanged for imidazole buffer (50 mM $NaPO_4$ buffer pH 7.5, 300 mM NaCl, 10 mM imidazole, 10% glycerol, 1 mM $MgCl_2$, 10 μM Mg-ATP) using protein desalting spin columns (Pierce) and loaded onto a Ni^{2+}-sepharose column (Amersham Biosciences HisTrap HP). The column was washed with imidazole buffer and the protein was eluted with a continuous imidazole gradient (10 mM—300 mM). Peak fractions were pooled, aliquoted and snap-frozen in liquid N_2. Protein was stored at –80 °C (His_6-Kip3p) or in liquid N_2 (His_6-Kip3-eGFP and His_6-eGFP-Kip3).

References

S1. Kalaidzidis, Y. L., Gavrilov, A. V., Zaitsev, P. V., Kalaidzidis, A. L. & Korolev, E. V. PLUK - an environment for software development. Program. Comput. Softw. 23, 206-211 (1997).